ISSN 1063-7842, Technical Physics, 2018, Vol. 63, No. 1, pp. 51–56. © Pleiades Publishing, Ltd., 2018.
Original Russian Text © Ya.A. Lyashenko, V.L. Popov, 2018, published in Zhurnal Tekhnicheskoi Fiziki, 2018, Vol. 88, No. 1, pp. 52–57.

PHYSICAL SCIENCE OF MATERIALS

Model of Nanostructuring Burnishing by a Spherical Indenter Taking into Consideration Plastic Deformations

Ya. A. Lyashenko[a,b] and V. L. Popov[a,c,d,*]

[a] *Berlin Technical University, Berlin, 10623 Germany*
[b] *Sumy State University, Sumy, 40007 Ukraine*
[c] *National Research Tomsk State University, Tomsk, 634050 Russia*
[d] *National Research Tomsk Polytechnic University, Tomsk, 634050 Russia*
**e-mail: popov@tu-berlin.de*

Received May 30, 2017

Abstract—A dynamic model of the nanostructuring burnishing of a surface of metallic details taking into consideration plastic deformations has been suggested. To describe the plasticity, the ideology of dimension reduction method supplemented with the plasticity criterion is used. The model considers the action of the normal burnishing force and the tangential friction force. The effect of the coefficient of friction and the periodical oscillation of the burnishing force on the burnishing kinetics are investigated.

DOI: 10.1134/S1063784218010188

1. INTRODUCTION

One of the relevant problems of modern engineering is the modification of physical properties of the surface [1]. There are many different methods applied to this modification, including ion implantation, laser processing, plasma processing, vacuum deposition, and many others. The goal of all of these methods is to modify the surface properties of the material in order to make them convenient for concrete engineering applications; it may be a product of a surface layer with a higher melting temperature, changed refraction index, reduced wear, increased plasticity (or hardness), corrosion resistance and many other characteristics. The main idea of the surface modification is the absence of a need to produce a whole detail of expensive material, since it only interacts with the environment (other objects) through its surface; thus, those are the contact (surface) properties that are important rather than the three-dimensional ones.

One of the most efficient and promising methods of surface modification is nanostructuring burnishing [2–4]. In the process of burnishing, an indenter (as a rule, spherical) is being plunged into the detail surface to the micrometer depths (one controls either the indentation depth or the acting normal force) and processes the detail, making several passes over it with a velocity of about 1 m/s. During this process, intensive plastic deformations appear in the contact zone and their action leads to the fragmentation of the detail surface layer and to the formation of structural defects, including the grain boundaries. With each passage of the indenter, the average grain size will tend to a concrete value depending on the plastic deformation values and on the temperature in the contact zone [5, 6]. As a result, the strength and plastic properties of the burnished detail become improved and the wear resistance is increased. The advantage of the nanostructuring burnishing method is its high efficiency with no need to use expensive equipment. An important point is that this method can be applied to burnishing details with holes [7].

Despite that the nanostructuring burnishing method is actively applied in industry, the processes that take place during burnishing are still far from completely understood. One of the developed theoretical lines of research of the burnishing process is based on computer modeling, which uses both the finite element method [8] and the movable cellular automation method [9]. Another line of research is the development of different phenomenological models [7, 10]. Even though phenomenological models cannot precisely describe all of the processes that take place while burnishing a detail, their undeniable advantage is the possibility of establishing the general regularities between the result of the process and the model parameters. For example, in [10], the estimated critical value of damping was found such that the self-oscillation regime stops when it is exceeded. It has a practical significance when burnishing details with holes, since when going out from a hole, the indenter

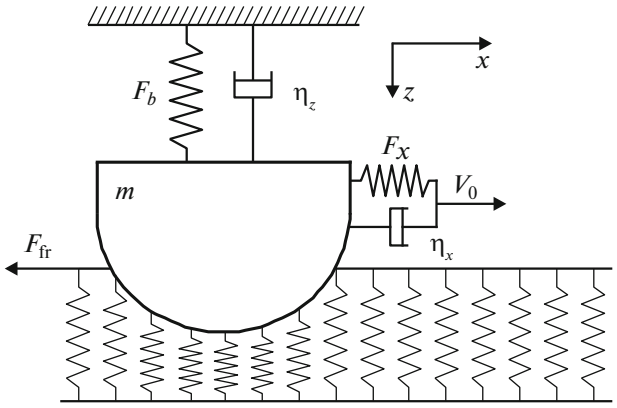

Fig. 1. Scheme of the movement of the indenter in the process of nanostructuring burnishing.

raises itself a little over the detail surface (gets out of the contact), after that, it is important for the system to attain a stationary burnishing regime for the least time possible, avoiding oscillations of indenter which would lead to deterioration of the detail surface [7]. In this work, based on the models [7, 10], we have suggested a model of nanostructuring burnishing with consideration of plastic deformations. To describe plastic deformations, the ideology of the dimension reduction method [11] was used together with the plasticity criterion [12].

2. FORMULATION OF THE MODEL IN TERMS OF MDR FORMALISM

Figure 1 schematically shows the process of nanostructuring burnishing. Here, a spherical indenter with a mass m slides over the detail surface (shown by springs) in the positive direction of the OX axis by means of the external drive with a constant velocity V_0. A normal force, the actin of which leads to the immersion of the indenter into the substrate, is designated as F_b (force of burnishing). The coefficient of damping in the normal direction is η. The moving drive and the indenter are connected by the Kelvin–Voigt model with the elastic force F_x and the damper η_x. When the indenter is moving, the friction force F_{fr} appears between its surface and the surface of the detail; this force is shown in Fig. 1. Let us write the equation of motion for an indenter moving in the normal direction. It will have the form [10]

$$m\frac{d^2z}{dt^2} + \eta_z\frac{dz}{dt} = F_b - F_n, \tag{1}$$

where F_n is the normal contact force acting from the detail's side. To determine the evolution of the contact force in the process of motion, we will use the method of dimension reduction (MDR) [11], which makes it possible to provide an exact description for concrete problems of axially symmetric bodies. In the context considered here, this method is not exact and, thus, the suggested analysis should be considered a qualitative analysis of basic laws of the process. Let us first consider the peculiarities of the MDR method without taking into account plastic deformation. Let the indenter be made of a material with the elasticity modulus E_1, rigidity modulus G_1, and the Poisson's ratio ν_1. Similar parameters for the burnished detail are E_2, G_2, and ν_2. It is known that this contact problem can be reduced to the problem of contact between an incompressible indenter and a half-space with elastic parameters E^* and G^* determined as

$$\frac{1}{E^*} = \frac{1-\nu_1^2}{E_1} + \frac{1-\nu_2^2}{E_2}, \tag{2}$$

$$\frac{1}{G^*} = \frac{2-\nu_1}{4G_1} + \frac{2-\nu_2}{4G_2}. \tag{3}$$

Next, it is necessary to discretize the half-space by representing it in the form of noninteracting springs with the normal and tangential rates

$$k_z = E^*\Delta x, \quad k_x = G^*\Delta x, \tag{4}$$

respectively, where Δx is the value of discretization (the distance between springs). Describing the process of the indentation of the indenter with an original three-dimensional profile $z = f(r)$ in the one-dimensional space, it is necessary to represent it in the form

$$g(x) = \int_0^{|x|} \frac{f(r)}{\sqrt{x^2 - r^2}}\,dr. \tag{5}$$

For a spherical indenter $f(r) = r^2/2R$, transformation (5) leads to the dependence $g(x) = x^2/R$. As a result, the individual spring tensions in the process of indentation into the half-space to depth d can be calculated as

$$u_z(x) = d - g(x) = d - \frac{x^2}{R}. \tag{6}$$

It is easy to find the contact radius a from relation (6). Thus, at $x \equiv a$ and $u_z(a) = 0$, we will have $a = \sqrt{Rd}$, which is certainly coincides with the classical solution. Knowing the indentation depth d, one can find the acting normal force F_n. With this purpose, it is necessary to summarize the tension forces from each spring in the contact as follows:

$$F_z(a) = E^*\int_{-a}^{a} u_z(x)dx = 2E^*\int_0^{\sqrt{Rd}}\left(d - \frac{x^2}{R}\right)dx = \frac{4E^*\sqrt{Rd^3}}{3}. \tag{7}$$

However, for the numerical modeling, one has to use a discrete representation of the integral, i.e., to use an expression in the form

$$F_z = E^*\Delta x\sum_{\text{cont}} u_z(x_i), \quad (8)$$

where the summation is carried out over the entire contact. As before, the function $u_z(x_i)$ is given by expression (6).

When processing a detail, an indenter moves horizontally, generating the friction force that also has an impact on the process of burnishing. The method of dimension reduction makes it possible to describe the friction force. It is known that, in the case when the materials of the indenter and the burnished surface have elastic similarity, i.e., when the condition

$$\frac{1-2\nu_1}{G_1} = \frac{1-2\nu_2}{G_2}, \quad (9)$$

is satisfied, the normal and tangential problems can be considered independently from each other.

Let us briefly describe the algorithm of modeling the tangential movement of the indenter in terms of the MDR method with a finite coefficient of friction μ. To consider sliding, it is necessary to verify the condition

$$\mu E^* u_z(x_i) \le |G^* u_x(x_i)|, \quad (10)$$

at each iteration for all springs. Here, $u_x(x_i)$ is the tangential displacement of springs at the contact. If condition (10) holds true, then the spring will slide. To include the consideration of sliding, it is necessary to add incrementally the displacement of the indenter to the horizontal displacement of springs at each step; then, condition (10) has to be verified for all springs. For the springs for which this condition is satisfied, a new displacement value is established

$$u_x(x_i) = \pm\frac{\mu E^* u_z(x_i)}{G^*}, \quad (11)$$

where the sign coincides with that of $u_x(x_i)$ before having set a new value to $u_x(x_i)$. Then, the tangential force (the friction force) F_{fr} is calculated according to the formula

$$F_{\text{fr}} = G^*\Delta x\sum_{\text{cont}} u_x(x_i). \quad (12)$$

This algorithm was previously used to describe the effect of ultrasound on the coefficient of friction [13]. This approach makes it possible to exactly describe the process of elastic deformation. However, in the process of burnishing, a detail is deformed plastically. Apparently, the description of the nonlocal plasticity is impossible in terms of the MDR. One of the reasons for this is that a contact is not axially symmetrical in the case of the tangential motion and in the presence of the plastic deformation. For example, in the problem shown in Fig. 1 (at a constant indention depth), the springs on the left side with respect to the contact center will undergo the maximum plastic deformations, whereas the springs on the right side will continue to be deformed. Thus, the normal force on the right side will be greater, which does not correspond to the MDR ideology. Therefore, one should understand the study carried out below not as an exact description of the process but as its modeling intended to describe possible regimes of nanostructuring burnishing.

In [12], the criterion of the plastic deformation was suggested, which we will use in our modeling. The normal force can be written in the form

$$F_n = \pi q_c a, \quad (13)$$

where a is the contact radius, q_c describes the critical linear density of the force whose exceedance leads to plastic deformations. The critical force f_c acting on one spring can be found as follows:

$$f_c = \frac{F_n}{2a/\Delta x}. \quad (14)$$

From (13) and (14), we obtain the following expression for f_c [12]:

$$f_c = \frac{\pi}{2} q_c \Delta x, \quad (15)$$

where f_c is the critical (maximum) elastic force, the exceedance of which causes the plastic sample deformation. Let us consider the algorithm for modeling the plastic deformation for a single spring. Let its compression be $u_z(x_i)$. The condition

$$u_z(x_i) \ge \frac{f_c}{E^*\Delta x} \quad (16)$$

is verified at each step. If (16) holds true, then a new value of the elastic spring tension $u_z'(x_i) = f_c/(E^*\Delta x)$ is established. The plastic indention depth will be $d_{\text{pl}} = u_z(x_i) - u_z'(x_i)$. At subsequent verifications, when condition (16) is satisfied with a new value $u_z'(x_i)$, the value d_{pl} will be accumulated. As a result of the passage of the indenter, we will obtain a plastic track whose shape is determined by a set of parameters of the dynamical system shown in Fig. 1.

3. MOTION OF THE INDENTER WITH A CONSTANT VELOCITY

First, let us consider a simplified case in which an indenter moves with a constant velocity V_0, which corresponds to the value $\eta_x \to \infty$ (Fig. 1). Physically, this situation corresponds to the motion of an indenter in the rigid guides [10] and is often realized in experiments. Nevertheless, it should be noted that the horizontal oscillations of the indenter will take place even in the case of using rigid guides; however, they can be neglected compared with the vertical oscillation amplitude. In this case, the friction force has no impact on the obtained profiles of burnished surfaces, since the horizontal coordinate grows linearly over time. However, the presence of the friction force is necessary directly in the experiment, since surface

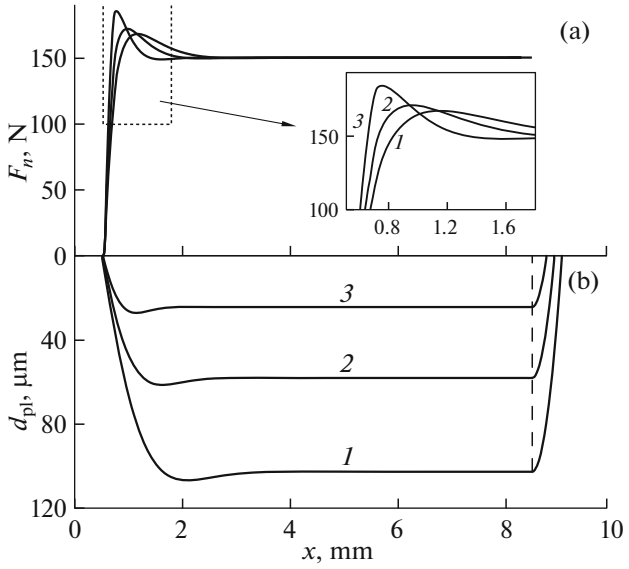

Fig. 2. (a) Dependences of the acting normal force F_n on the indenter horizontal coordinate x; (b) plastically deformed profile of a steel detail after a single pass by a diamond indenter. Both figures are plotted at parameters R = 3 mm, F_b = 150 N, v_x = 2 m/s, m = 30 g, η_z = 30 kg/s; curves *1–3* refer to values $\pi q_c/2 = 2.5 \times 10^5$, 3.2×10^5, 4.5×10^5 N/m.

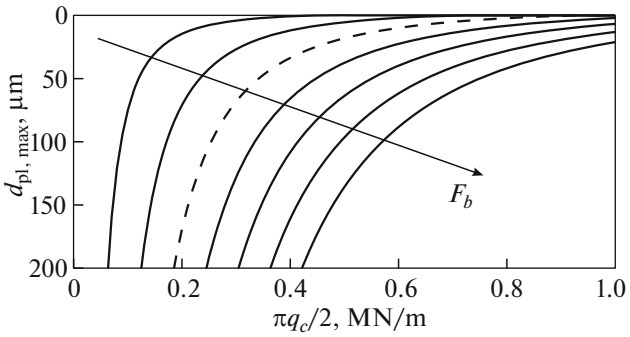

Fig. 3. Dependences of the stationary value of the plastic track depth $d_{pl,\,max}$ on the parameter q_c, plotted at the same parameters as in Fig. 2. Values of the burnishing force F_b grows from 50 to 350 N with a step of 50 N (the direction of increasing of the force F_b is shown by an arrow). Dashed line refers to the value F_b = 150 N, as in Fig. 2.

layer deformation is only observed in this case, which is the aim of burnishing.

Figure 2 presents the results of modeling at fixed model parameters. For the numerical calculations, the discretization parameters were chosen as $\Delta x = 10^{-7}$ m and $\Delta t = 10^{-7}$ s and Eq. (1) was solved by the Euler method. The calculations were carried out up to the moment $t_{max} = 4$ ms (this moment of time corresponds to the ends of dependences in Fig. 2a). The results shown in Fig. 2 correspond to burnishing a steel surface ($E_2 = 2.08 \times 10^{11}$ Pa, $\nu_2 = 0.3$) by a diamond indenter ($E_1 = 11.472 \times 10^{11}$ Pa, $\nu_1 = 0.2$). It follows from Fig. 2 that, over time, the system attaints a stationary operation regime at which the normal contact force F_n is equal in magnitude to the burnishing force F_b. In addition, the indention depth is reduced as the critical density of the force q_c grows. The value q_c is a characteristic of the material, so it is difficult to vary it. However, it should not be forgotten that the indentation depth can be easily increased by increasing the value of the burnishing force F_b. It is necessary to take into account that the friction force F_{fr} will grow proportionally to the increase in the normal force (since the contact area grows), so the dissipation of mechanical energy will also increase, which can result in the melting of the metal in the contact zone or to its fracturing. This imposes considerable constraints on the value of the burnishing force; therefore, the effect of all parameters (the normal force, coefficient of friction, indenter mass, etc.) should be considered in complex and the suggested model allows us to do it. The curves in Fig. 2 do not start from the origin of coordinates, since the initial coordinate of the indenter center is chosen as $x_0 = 0.5$ mm. The ends of the dependences in Fig. 2a correspond to the indenter stopping and the calculations are no longer performed. Therefore, beginning from the coordinate at which the dependences in Fig. 2a come to an end, the plastic track depth d_{pl} in Fig. 2b begins to decrease until attaining zero (the detail surface which does not undergo processing). At all dependences $d_{pl}(x)$, the minimum (the hollow) is realized before attaining the stationary regime of burnishing. This hollow often takes place in experiments, which results in the self-oscillation regime of burnishing as the detail surface undergoes multiple processing [10]. Such a regime can be described also in terms of the considered model; however, its investigation goes beyond the goal of this work. We performed This study in detail in [10].

Since the main goal of this study is investigation of plastic effects, in Fig. 3, we present additional dependences of the stationary value of the plastic track depth $d_{pl,\,max}$ on the parameter q_c that specifies plastic properties of the burnished detail. It can be seen from Fig. 3 that, with increasing q_c, the track depth of all curves decreases until zero (elastic deformation of the sample is attained in the absence of plastic deformation).

4. EFFECT OF THE FRICTION FORCES

As was noted above, the indenter motion with a constant velocity is an idealization of the process of burnishing. So, let us consider the case when we fix the driving force (F_x = const) instead of the velocity. In this situation, the considerable effect on the process of burnishing is caused by the friction force F_{fr}, since it will change as the indenter is moving in the normal

direction. To describe the dynamics of this process, it is necessary to complete the equation for the normal coordinate $z(1)$ using a similar equation that describes the motion of the indenter in the horizontal direction. Taking into account all acting forces, this equation takes the form

$$m\frac{d^2x}{dt^2} + \eta_x \frac{dx}{dt} = F_x - F_{\text{fr}}. \quad (17)$$

It is worth mentioning that kinetic equations (1) and (17) are not independent, since the friction force F_{fr} (Eq. (17)) is a function of the normal force F_n (Eq. (1)). The results of modeling are shown in Fig. 4 (the duration of the process of burnishing for all curves is identical, $t_{\max} = 25$ ms). The parameters G_1 and G_2 used in modeling the effect of the friction force were calculated according to the known relation

$$G_{1,2} = \frac{E_{1,2}}{2(1+\nu_{1,2})}. \quad (18)$$

Curves *1–5* in Fig. 4 show that for the same period of time at a fixed driving force F_x, the displacement of the indenter in the tangential direction is smaller when the coefficient of friction μ is greater. Curve *6* is plotted at the coefficient of friction $\mu = 0.4$, at which sliding is absent and static friction is realized. Therefore, sliding (tangential movement) is absent here and the plastic deformation is only observed in the zone of the initial contact. As the coefficient of friction grows further, the dependences $d_{\text{pl}}(x)$ repeat the shape of curve *6*. It should be noted that, in fact, the coefficient of friction in the diamond–still pair is about 0.1; however, we carry out the calculations for larger values of the coefficient of friction because an indenter can be made from different materials and the value of the coefficient of friction plays the determining role in the process of burnishing. If the coefficient of friction is lower than the critical value, then the surface layer of the detail will not be deformed plastically; hence, one of the important aspects in the technological process of nanostructuring burnishing is to ensure a high coefficient of friction.

5. EFFECT OF PERIODICAL OSCILLATION OF THE NORMAL FORCE

To ensure the required operation regime, one often applies external periodical action to the indenter. This action can, e.g., reduce the friction force [12] and even create an ordered motion of friction surfaces [14]. In our case, the external periodical action can be describe using the oscillations of the burnishing force F_b in the form

$$F_b = \tilde{F}_b + \tilde{F}\cos(2\pi\tilde{\nu}t). \quad (19)$$

Figure 5 presents the results of modeling at such a dependence of the normal force. The value of $\tilde{F}_b$ is chosen equal to the value of the burnishing force at

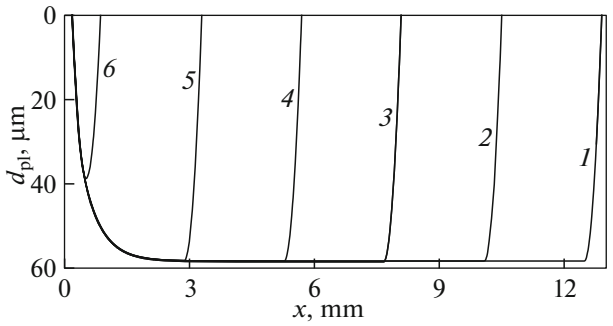

Fig. 4. Plastically deformed profile of a steel detail after the procedure of burnishing at parameters like in Fig. 2 and $\pi q_c/2 = 3.2 \times 10^5$ N/m, $G_1 = 4.78 \times 10^{11}$ Pa, $G_2 = 8 \times 10^{10}$ Pa, $\eta_x = 30$ kg/s, $F_x = 60$ N. Curves *1–6* refer to $\mu = 0.3, 0.32, 0.34, 0.36, 0.38, 0.4$.

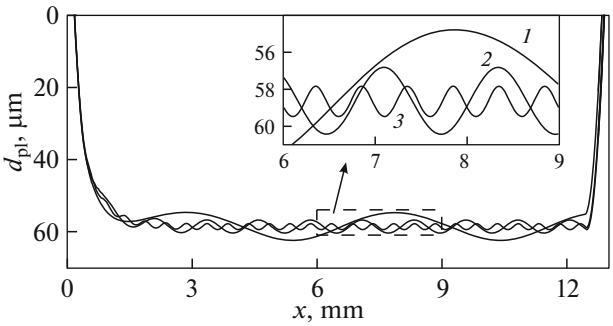

Fig. 5. Plastically deformed profile of a steel detail at parameters like those in Fig. 4, $\mu = 0.3$, $\tilde{F}_b = 150$ N, and $\tilde{F} = 5$ N. Curves *1–3* refer to frequencies $\tilde{\nu} = 100$, 400, and 1000 Hz.

which previous figures were plotted. Therefore, the average value of the force $\langle F_b \rangle$ at which a burnishing device acts on the indenter does not change. It follows from Fig. 5 that the waviness amplitude of the burnished surface decreases as the frequency increases. In the limit $\tilde{\nu} \to \infty$, the burnished surface will be smooth like in Fig. 4.

Figure 6 demonstrates the dependences of the oscillation amplitude for the plastic track $d_{pi}(x)$ shown in Fig. 5 in the stationary burnishing regime. All parameters in Figs. 5 and 6 are similar; it is only the value of the damping coefficient η_z that changes, its increase is shown by an arrow. It follows from Fig. 6 that the waviness amplitude A_{pl} decreases as the frequency $\tilde{\nu}$ grows. The waviness amplitude also decreases, albeit insignificantly, as the damping coefficient grows. It is shown in [10] that, as the damping coefficient exceeds the critical value, the self-oscillation regime is suppressed. However, unlike [10], where the normal force remained fixed and the oscillations were performed due to the presence of holes in the detail, here, we

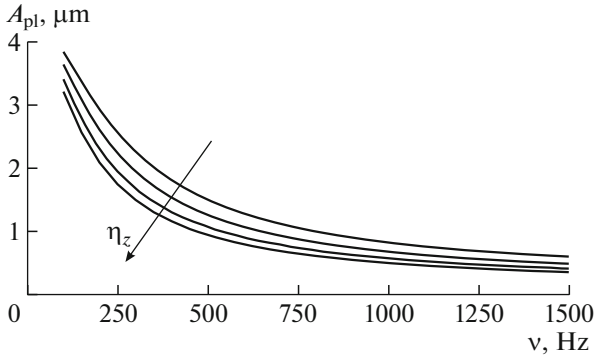

Fig. 6. Amplitude of oscillations of the plastic track A_{pl} shown in Fig. 5 as a function of the frequency of the change in the normal force $\tilde{\nu}$. Curves shown in Fig. 6 refer to the values $\eta_z = 30$, 250, 500, and 700.

consider external oscillations of the normal force. As can be seen, a considerable increase in the damping coefficient insignificantly reduces the oscillation amplitude.

It worth mentioning that this periodical change in the value of the normal force in the process of burnishing may occur due to the presence of holes in the detail which are arranged in a row along the passage of the indenter. As one can see, the effect of the periodical action in a wide range of parameters results in the waviness of the burnished detail. One of the principal possibilities of avoiding this effect is the construction of intellectual systems that would control the advance of the indenter while changing the normal burnishing force, thereby ensuring its constant value. In this case, it becomes possible to burnish surfaces with holes or irregularities.

It should be noted that the described burnishing regime with waviness can also have a positive effect. In the case of an internal combustion engine or hydraulic systems, this regime can be used to make grooves with micrometer-scale depths at the surface of a piston moving in the cylinder and those grooves can be filled with lubricant.

6. CONCLUSIONS

In this work, we have suggested a simple model that makes it possible to carry out numerical modeling for the dynamic process of nanostructuring burnishing. In terms of this model, the contact radius, normal and tangential contact forces, plastic track after burnishing, as well as the indenter position in space and the velocity of its motion can be determined. Using this model, the effect of the friction force on the dynamics of the process is analyzed and it has been shown that the increase in the coefficient of friction results in the reduction of the velocity of the indenter motion at a fixed tangential driving elastic force. The study of the effect of imposed indenter oscillations in the normal direction has shown that, with an increase in the oscillation frequency, the burnished surface approaches to the smooth one. The model we proposed can be used for further studying the process of burnishing, namely, for studying the effect of oscillations in the tangential direction, determining the effect of the indenter shape (the used method enables modeling for any axially symmetrical shape of the indenter). The model can be easily generalized to burnishing viscoelastic details and to gradient media; it is possible to consider the adhesion between contacting surfaces.

ACKNOWLEDGEMENTS

This work is supported by the German Research Foundation (DFG), the Ministry of Education and Science of the Russian Federation, and the program of competitive recovery of Tomsk State University. Ya. A. Lyashenko acknowledges the support of the Ministry of Education and Science of Ukraine (project no. 0116U006818).

REFERENCES

1. A. D. Pogrebnjak, S. N. Bratushka, V. M. Beresnev, and N. Levintant-Zayonts, Russ. Chem. Rev. **82**, 1135 (2013).
2. A. M. Hassan and A. S. Al-Bsharat, Wear **199**, 1 (1996).
3. M. Korzynski, Int. J. Mach. Tools Manuf. **47**, 1956 (2007).
4. S. Swirad, Wear **271**, 576 (2011).
5. A. V. Khomenko, Ya. A. Lyashenko, and L. S. Metlov, Metallofiz. Noveishie Tekhnol. **30**, 859 (2008).
6. L. S. Metlov, M. M. Myshlyaev, A. V. Khomenko, and Ya. A. Lyashenko, Tech. Phys. Lett. **38**, 972 (2012).
7. V. P. Kuznetsov, S. A. Il'ichev, and V. G. Gorgots, Russ. Eng. Res. **29**, 1148 (2009).
8. V. P. Kuznetsov, I. Yu. Smolin, A. I. Dmitriev, D. A. Konovalov, A. V. Makarov, A. E. Kiryakov, and A. S. Yurovskikh, Phys. Mesomech. **16**, 62 (2013).
9. V. P. Kuznetsov, S. Yu. Tarasov, and A. I. Dmitriev, J. Mater. Process. Technol. **217**, 327 (2015).
10. Ya. A. Lyashenko, V. P. Kuznetsov, M. Popov, V. L. Popov, and V. G. Gorgots, Fiz. Mezomekh. **18** (1), 38 (2015).
11. V. L. Popov and M. Heβ, Method of Dimensionality Reduction in Contact Mechanics and Friction (Springer, Berlin, 2015).
12. V. L. Popov, Facta Univ., Ser.: Mech. Eng. **13**, 39 (2015).
13. E. Teidelt, V. L. Popov, and J. Starcevic, Tribol. Lett. **48**, 51 (2012).
14. T. H. Cheng, M. He, H. Y. Li, X. H. Lu, H. W. Zhao, and H. B. Gao, IEEE Trans. Ind. Electron. **64**, 5545 (2017). doi 10.1109/TIE.2017.2677318

Translated by E. Smirnova